Effect of bound dineutrons upon big bang nucleosynthesis

James P. Kneller* and Gail C. McLaughlin†
Department of Physics, North Carolina State University, Raleigh, North Carolina 27695-8202, USA
(Received 9 January 2004; published 17 August 2004)

We have examined the effects of a bound dineutron ^2n upon big bang nucleosynthesis (BBN) as a function of its binding energy B_{2_n}. We find a weakly bound dineutron has little impact but as B_{2_n} increases its presence begins to alter the flow of free nucleons to helium-4. Because of this disruption, and in the absence of changes to other binding energies or fundamental constants, BBN sets a reliable upper limit of $B_{2_n} \lesssim 2.5$ MeV in order to maintain the agreement with the observations of the primordial helium-4 mass fraction and D/H abundance. We also consider simultaneous variations in B_{2_n} and the deuteron binding energy B_D using a simplified BBN calculation. We demonstrate that only when B_D is very close to 1.7 MeV does the B_{2_n} upper limit increase to 3.5 MeV, a value set by incompatibility of an observed primordial $A=2$ abundance with the decay of deuterons.

DOI: 10.1103/PhysRevD.70.043512 PACS number(s): 98.80.Ft, 21.10.Dr, 26.35.+c

I. INTRODUCTION

The concordance of the predicted synthesis of the lightest nuclei during the period immediately following the big bang with the observed primordial abundances presents us with a powerful probe of the state of the Universe during its earliest epochs. In addition to constraining standard cosmological parameters such as the density of baryons, the number of neutrino flavors and their degeneracy [1–15] big bang nucleosynthesis (BBN) is sufficiently complex that one can also learn about such possibilities as quintessence [16–19], modifications of gravity [19,20] or neutrino oscillations, neutrino mass, or neutrino decay [21–29].

Perhaps the most intriguing use of BBN is in constraining the variation of the fundamental constants [30–38]. Support for this hypothesis has emerged from recent observations of quasar absorption lines at redshift of $z=1-2$ by Webb *et al.* [39,40] that suggest the fine structure constant, α, may have been smaller in the past (though see [41,42]). In some cases the variation of a fundamental constant is easily implemented in BBN because the nuclear physics aspects of the calculation are unaffected, but in others the lack of an adequate theory to predict such properties as the nuclear binding energies and cross sections introduces a degree of uncertainty. Nevertheless, one can derive limits to any variation in these circumstance by simply requiring, for example, the deuteron to be stable as in Barrow [31], or attempt to determine the scale of the uncertainties as in the calculation of Kneller and McLaughlin [38].

In addition to variation of the properties of nuclei that are presently stable, variation of the constants relevant to nuclear structure might also partially stabilize nuclei that are presently particle unstable. This could have pronounced effects upon BBN because, for example, the lack of any stable $A=5$ and $A=8$ nuclei is often cited as the explanation for the dearth of nuclei formed with masses above helium-4 though the endothermicity of pure strong reactions such as $^4\mathrm{He}(T,n)^6\mathrm{Li}$, $^4\mathrm{He}(^4\mathrm{He},p)^7\mathrm{Li}$ and $^4\mathrm{He}(^4\mathrm{He},n)^7\mathrm{Be}$ plays a role.

The focus in this paper is upon another nucleus that could also become stabilized—the dineutron ^2n. The dineutron, a member of the nucleon-nucleon isospin triplet, is a spin singlet and, by itself, the dineutron is weakly unbound[1] by $\sim$70 keV, the *n*-*n* scattering length being negative [43–46]. Early direct searches [47] did not see evidence for a stable dineutron but recently Bochkarev *et al.* [48] claim that $45\pm10\%$ of the decay of an excited state of ^{6}He is through the dineutron[2] and Seth and Parker [50], amongst others, find evidence for dineutrons in ^{5}H, ^{6}H and ^{8}He decay. There is also a claim for tetraneutron, ^4n, emission in the decay of ^{14}Be [51].

Given that the dineutron is only weakly unbound, even small changes in the pion mass could, perhaps, result in a bound dineutron, although at present there is not enough experimental information to show whether or not this would occur [52,53]. The scattering length is quite sensitive to the pion mass and so it is small changes in fundamental constants that change its mass, such as α, Λ_{QCD} or the Higgs vacuum expectation value (VEV), that could cause the dineutron to become bound. Since we are lacking an exact relationship between these fundamental constants and the binding energy of the dineutron we do not adopt a particular model for the time variation of fundamental constants, but instead explore the effect upon BBN of a bound dineutron directly.

In this paper we shall make an effort to derive a constraint upon the dineutron binding energy. Initially we will consider the dineutron in isolation, i.e. whatever the source of the new stability of the dineutron we shall limit the effect to just this nucleus. We begin with an overview of standard BBN in Sec. II with an emphasis on the details of the flow from free nucleons to helium-4 before proceeding to insert dineutrons

*Electronic address: Jim_Kneller@ncsu.edu
†Electronic address: Gail_McLaughlin@ncsu.edu

[1]Though it may become stable on the surface of neutron-rich nuclei.

[2]Bochkarev *et al.* [49] also have evidence of diproton emission from an excited state of ^{6}Be.

in Sec. III. In Sec. IV we present our results for a baryon-to-photon ratio of $\eta=6.14\times10^{-10}$ and follow it up in Sec. V with a discussion of the errors in the calculation and any degeneracy with η in Sec. VI. Finally, in Sec. VII, we show how BBN can limit the dineutron binding energy before discussing simultaneous variations of both dineutron and deuteron binding energies in Sec. VIII and then present our conclusions.

II. BBN WITHOUT DINEUTRONS

BBN can be simplistically broken into three phases characterized by the degree of equilibrium within the nucleons or nuclei.

During the first phase, at temperatures above $T\gtrsim1$ MeV, there are virtually no complex nuclei so that all the nucleons exist in a free state. The rapidity of the weak interactions in converting neutrons and protons,

$$n\leftrightarrow p+e+\overline{\nu_e} \tag{1a}$$

$$n+\overline{e}\leftrightarrow p+\overline{\nu_e}, \tag{1b}$$

$$n+\nu_e\leftrightarrow p+e, \tag{1c}$$

establish a weak equilibrium so that the neutron to proton ratio, F, is simply $F\approx\exp(-\Delta_{\rm np}/T)$. As the Universe cools the rate at which neutrons must be converted to protons in order to maintain the equilibrium cannot be accommodated. As a consequence, the neutron-to-proton ratio departs from its equilibrium value and is said to ''freeze-out'' even though conversion continues to occur. In the absence of neutron decay and the formation of complex nuclei, the ratio would attain an asymptotic value of $F\sim1/6$ [69,70]. The departure of F from its equilibrium value denotes the boundary between the first two phases of BBN.

During the second phase of BBN, from a temperature of ~1 MeV to ~100 keV, the abundances of the various nuclei also begin to depart from equilibrium. At ~1 MeV their abundances are suppressed relative to the free nucleons but the nuclear reactions that form them establish, and maintain, chemical or nuclear statistical equilibrium (NSE). In equilibrium the abundance,[3] $Y_A=n_A/n_B$, of a complex nuclei A is derived from $\mu_A=Z\mu_p+(A-Z)\mu_{\rm n}$ so after inserting the expressions for the Boltzmann number density we find

$$Y_A=\frac{g_A A^{3/2}}{2^A}\left[n_B\left(\frac{2\pi}{m_N T}\right)^{3/2}\right]^{A-1}Y_{\rm p}^{Z}Y_{\rm n}^{A-Z}e^{B_A/T}. \tag{2}$$

Using $F\sim1/6$ and a baryon-photon ratio of $\eta\sim10^{-10}$ we see that for a temperature of T~1 MeV the abundance of deuterons is $Y_{\rm D}\sim10^{-12}$. After substituting $Y_{\rm D}$ for the thermal factors in Eq. (2) we obtain

$$Y_A=\frac{g_A A^{3/2}}{2[3\sqrt{2}]^{A-1}}Y_{\rm p}^{1+Z-A}Y_{\rm n}^{1-Z}Y_{\rm D}^{A-1}\times\exp\left(\frac{B_A-(A-1)B_{\rm D}}{\rm T}\right). \tag{3}$$

This equation now makes it much clearer that the abundance of a nucleus with mass $A+1$ is suppressed by approximately $Y_{\rm D}$ relative to the abundance of a nucleus with mass A.

If the neutron or proton abundances are held fixed then the NSE abundance has a minimum at $T_A=2B_A/(3A-3)$. Below T_A the various nuclear reactions provide sufficient nuclei to keep Y_A in equilibrium as the abundance climbs from the minimum but eventually a point is reached where this required production rate cannot be met and the abundance falls beneath the equilibrium value. This departure from equilibrium for the complex nuclei is in contrast with that of the neutrons where it was an insufficient rate that led to the departure, here it is a lack of reactants that is the cause. Heavier nuclei are the first to depart from equilibrium: helium-4 departs at $T\sim600$ keV while helium-3 and tritium drop out at $T\sim200$ keV. Below $T\sim200$ keV the only compound nucleus in NSE is the deuteron and its abundance controls the rate at which all the heavier nuclei can be produced. By $T\sim100$ keV the D abundance is approaching that of the free nucleons and the amount of D destruction, via such reactions as D(D,p)T and D(D,n)^{3}He, has become significant. When this occurs the deuteron abundance cannot be replenished sufficiently quickly to maintain its equilibrium and, consequently, it too departs from NSE. This final NSE departure forms the entrance to the third stage of BBN proper.

Below the deuteron NSE departure temperature the D abundance continues to grow for a short period but eventually the D+D drain tips the balance in favor of destruction and the deuteron abundance reaches a peak amplitude. The tritons and helions formed via the reactions D(D,p)T and D(D,n)^{3}He are produced in roughly equal amounts but the helions rapidly transform to tritium via ^{3}He(n,p)T. The last step in the formation of the alpha particle is almost exclusively T(D,n)^{4}He which destroys $\sim1/3$ of all the deuterons formed. The essential steps in the scheme are illustrated in Fig. 1.

Smith, Kawano and Malaney [54] identified 8 reactions among the $A\leqslant4$ nuclei as being important for BBN. Five are identical to those in Fig. 1, the sixth is neutron-proton interconversion, and the two reactions they included, and which we have omitted from the figure, are ^{3}He(D,p)^{4}He and T(p,γ)^{4}He both of which are 2–4 orders of magnitude smaller than T(D,n)^{4}He, so their importance is marginal. Whatever the exact number, this handful (or two) of important reactions is much smaller than the number of reactions included in any BBN code.

As the Universe cools eventually the Coulomb barriers in the various reactions become insurmountable leading to a cessation of the nucleosynthesis. The abundances have plateaued to their ''primordial'' values with virtually every neutron now incorporated in helium-4 and only small residues in

[3]The term ''abundance'' is also used for the ratio Y_A/Y_H.

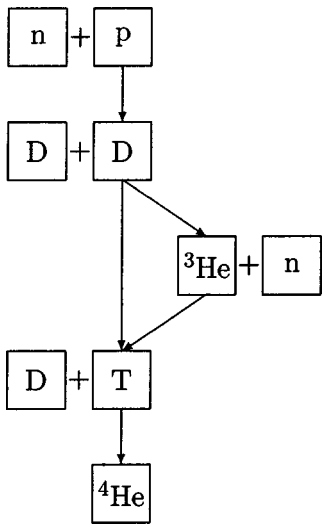

FIG. 1. A diagrammatic flow of nuclei in standard BBN. The complex nuclei are immersed in a (rapidly drained) bath of free nucleons and so we outline only where they form part of the set of reactants.

D, T and ^{3}He. A small (but detectable) abundance of lithium-7 and beryllium-7 have also been formed but we will not discuss these two nuclei further.

III. INSERTING DINEUTRONS INTO BBN

Inclusion of a new, light nucleus into BBN has the potential to significantly influence BBN and alter the predicted primordial abundances. These changes will occur because the dineutron will disrupt the flow of nucleons through the reaction network by both presenting new exit channels for reactions that already exist in BBN and through new entrance channels in the formation of the nuclei. One can construct a large number of plausible reactions in which dineutrons participate but not all are expected to play a prominent role for the same reason that standard BBN is dominated by only a few reactions. We can use our understanding of the important reactions in standard BBN to pick from the plethora of possibilities for dineutron reactions those which we expect to be important. The most important reactions involving dineutrons should be

preferably exothermic,
dominated by the strong interaction,
and two-bodied in their entrance channel.

Exothermicity plays a pivotal role in the BBN because, during its second two phases, the system does not attain an equilibrium and, typically, the flow of nuclei in any given reaction is in one direction. In a few cases where the Q value for the reaction is less than few times the temperature during BBN (i.e., $T\sim 100$ keV, $Q\sim 500$ keV) flow may be in both directions because the ''activation energy'' for an endothermic reaction is readily available. Examples of this behavior were seen in Kneller and McLaughlin [38]. The reaction should also be preferably strong in nature since this is the behavior seen in standard BBN where reactions such as $\mathrm{D}(\mathrm{D},n)^3\mathrm{He}$ dominate over $\mathrm{D}(p,\gamma)^3\mathrm{He}$ though, in a few cases, such as $p(n,\gamma)\mathrm{D}$, electromagnetic or weak interactions play an important role. The last requirement will remove those cases that pass the first two but whose entrance channels involve multiple particles.

From these requirements we have selected four dineutron reactions that we expect to be important:

$$p+{}^2n\leftrightarrow \mathrm{D}+n,\quad Q=2.22\ \mathrm{MeV}-B_{2_\mathrm{n}}, \tag{4}$$

$$\mathrm{D}+{}^2n\leftrightarrow \mathrm{T}+n,\quad Q=6.26\ \mathrm{MeV}-B_{2_\mathrm{n}}, \tag{5}$$

$$^3\mathrm{He}+{}^2n\leftrightarrow {}^4\mathrm{He}+n,\quad Q=28.29\ \mathrm{MeV}-B_{2_\mathrm{n}}, \tag{6a}$$

$$^3\mathrm{He}+{}^2n\leftrightarrow \mathrm{T}+\mathrm{D},\quad Q=2.99\ \mathrm{MeV}-B_{2_\mathrm{n}}. \tag{6b}$$

The dineutron binding energy will determine the Q value in these reactions and, if we permit values of B_{2_n} of several MeV, both Eqs. (4) and (6b) may reverse sign and Eq. (5) will become small. We will not consider any changes to the other nuclear binding energies. Though one may expect a large change in the dineutron binding energy to be reflected in equally significant changes to the structure of the deuteron, the effects upon three nucleon nuclei may be considerably smaller [55]. In our study, we also do not consider reactions leading to the formation of destruction of nuclei above mass 4.

To this list we add three additional reactions:

$$n+n\leftrightarrow {}^2n+\gamma,\quad Q=B_{2_\mathrm{n}}, \tag{7}$$

$$^2n\leftrightarrow \mathrm{D}, \tag{8}$$

$$^2n+p\leftrightarrow \mathrm{T}+\gamma,\quad Q=8.48\ \mathrm{MeV}-B_{2_\mathrm{n}}. \tag{9}$$

These reactions could become important for producing and, more importantly, removing dineutrons. In particular, the inclusion of Eqs. (8) and (9) is based on the following reasoning. Once we have dineutron cross sections we must integrate them over a Maxwell-Boltzmann spectrum to obtain a thermally averaged rate [56]. In all the dineutron reactions the lack of a Coulomb barrier means that the cross section for an exothermic reaction varies as $1/\sqrt{E}$ at low energy and so the rate becomes a constant. This can have important consequences: written in terms of the temperature, a reaction such as $A+B\rightarrow X$, with a rate per particle pair Γ, destroys nucleus A at a rate

$$\frac{dY_A}{dT}\propto \Gamma Y_A Y_B \tag{10}$$

where we have used the relations $n_B\propto T^3$ and $T^2\propto 1/t$. If we assume the abundance of nucleus B is much larger than A's and does not change by any other process then the solution to this equation is $Y_A\propto\exp(\Gamma Y_{B0}T)$ where Y_{B0} is the abundance of B at some fiducial temperature. In this scenario, the abundance of A never becomes a constant and BBN would never end. In standard BBN this situation never arises because the two temperature-independent reactions, $p(n,\gamma)\mathrm{D}$ and $^3\mathrm{He}(n,p)\mathrm{T}$, are killed by the decay of the neutron. But if the

dineutron becomes stable then without a reaction such as $^2n(p,\gamma)$T the dineutron abundance could plateau to a constant larger than, say, the abundance of helium-3 and the circumstances of Eq. (10) may be realized in the reaction ^{3}He$(^2n,n)^4$He. In order to obtain a primordial abundance of ^{3}He it is imperative that this situation be prevented. The decay of the dineutron and $^2n(p,\gamma)$T will ensure this by depleting the final dineutron abundance for all values of B_{2_n} we shall explore.

Now that we have determined the most important reactions, we need cross sections for them before we can proceed.

$^2n(p,n)$D, D$(^2n,n)$T, ^{3}He$(^2n,n)^4$He and ^{3}He$(^2n,$D$)$T

Since the dineutron is presently unstable we posit cross sections based on ''similar'' strong reactions involving deuterium or other light nuclei. If we consider an arbitrary two-body strong reaction $i+j\leftrightarrow k+l$ then general considerations lead us to expect a cross section per particle pair which is proportional to a matrix element squared, the phase space with an energy conserving delta function and inversely proportional to a flux. In nuclear astrophysics, one typically writes the cross section as

$$\sigma(E)=\frac{S(E)}{E}\exp\left(-\pi\alpha Z_i Z_j\sqrt{\frac{2\mu_{ij}}{E}}\right), \tag{11}$$

where μ_{ij} is the reduced mass for incoming particles i and j, and $S(E)$ is the astrophysical S-factor. For our purposes, this parametrization is not sufficient since it does not explicitly show the effects of a Q value upon the final states. This is particularly crucial since in our study Q values will vary as the dineutron binding energy varies. With that in mind, we write the non-resonant (S-wave) contributions to the cross section, following [57,58], as proportional to the product of both Coulomb penetrability factors $G_{ij}(E)$ and $G_{kl}(E+Q)$, the available phase space in the exit channel $\Phi_{kl}(E+Q)$ together with the statistical weight g_{kl} and the reciprocal of the entrance channel velocity. The penetrability factor for charged particle interactions, $G_{ij}(E)$, is simply

$$G_{ij}(E)=\sqrt{\frac{E_{ij}^C}{E}}\exp\left(-\pi\alpha Z_i Z_j\sqrt{\frac{2\mu_{ij}}{E}}\right), \tag{12}$$

where E_{ij}^C is the Coulomb barrier energy [59]. Although in the standard cross section parametrization, shown in Eq. (11), the second Coulomb penetrability factor can be absorbed into the astrophysical S factor because, typically, the energy is much smaller than the Q value, here we retain it explicitly. The phase space factor, $\Phi_{kl}(E+Q)$, is

$$\Phi_{kl}(E+Q)\propto\sqrt{(E+Q)\mu_{kl}^3} \tag{13}$$

while the statistical weight factor g_{kl} accounts for the multiplicity of the final state

$$g_{kl}=(2J_k+1)(2J_l+1) \tag{14}$$

where J_k and J_l are the spins of the individual nuclei. The reciprocal of the entrance channel velocity is proportional to $\Phi_{ij}/(\mu_{ij}E)$. Putting all these together the cross section for the reactions $i+j\leftrightarrow k+l$ is expected to be of the form

$$\sigma_{i+j\to k+l}(E)=S_{ij,kl}(E)\frac{g_{kl}}{\mu_{ij}E}G_{ij}(E)G_{kl}(E+Q)\times\Phi_{ij}(E)\Phi_{kl}(E+Q), \tag{15}$$

where we have introduced $S_{ij,kl}(E)$ as an undetermined function. This function becomes constant at low energy, and is similar to, but not the same as, the astrophysical S factor.

With the help of Eq. (15) we can extract the most obvious behavior of any cross section with energy to derive $S_{ij,kl}(E)$. Our expectation is that this quantity varies slowly though of course the exact details of a reaction may lead to significant departures. After extracting $S_{ij,kl}(E)$ from some known reaction we can then insert it into the similar dineutron reaction based on the assumption that $S_{ij,kl}$ does not change considerably from one to the other. The major changes in the cross sections will therefore be limited to the considerable effects of the Coulomb barrier penetrability and phase space. We have examined the validity of this approach by using it to predict D(D,p)T from D(D,n)^{3}He, and T(D,n)^{4}He from ^{3}He(D,p)^{4}He. The last two cross section are dominated by large resonances corresponding to excited states of ^{5}He and ^{5}Li [62] but the non-resonant pieces have been extracted by Chulick *et al.* [60] allowing us to compare the transformation. In both test cases we find the transformation works reasonably well with an error that is a factor of order a few.

For the $^2n(p,n)$D reaction there is no similar deuteron reaction with which to compare so instead we used the broadly similar ^{3}He(n,p)T. We have been unable to find an analytic expression for this cross section so we interpolated the ENDF-IV evaluated cross section data available online [61] and then factored out the expected behavior shown in Eq. (15) before replacing it with the appropriate terms for $^2n+p\leftrightarrow$D$+n$.

We expect the D$+^2n\leftrightarrow$T$+n$ cross section to be similar to D(D,p)T and D(D,n)^{3}He up to corrections for the Coulomb barrier penetrability and phase space factors. Here we have analytic expressions of the S factor to use from Chulick *et al.* [60].

To estimate the last two reactions, ^{3}He$+^2n\leftrightarrow n+^4$He and ^{3}He$+^2n\leftrightarrow$D$+$T, one appeals to their similarity with T(D,n)^{4}He so that one may use the Chulick *et al.* [60] expression and, once again, correct for the change in the phase space, Coulomb barrier penetrability etc. As mentioned earlier, the T(D,n)^{4}He cross section exhibits a resonance due to an excited state of the ^{5}He nucleus (see [62] for an energy level diagram). The position of this same resonance, relative to the ^{3}He$+^2n$ ground state, depends on the dineutron binding energy being subthreshold for $B_{2_n}\lesssim 3$ MeV. In addition, there are further excited states of ^{5}He that become relevant when $B_{2_n}\sim 0$ but, as we will show, the effects of the dineutron become apparent only when B_{2_n} approaches B_D and we have not added them to our cross section.

$$^2n \leftrightarrow \mathrm{D}$$

This weak reaction is actually the sum of *four* subprocesses:

$$^2n \leftrightarrow \mathrm{D} + e + \bar{\nu}_e, \quad 0 \leqslant E_\nu \leqslant \Delta_{^2\mathrm{nD}} - m_e, \tag{16a}$$

$$^2n + \nu_e \leftrightarrow \mathrm{D} + e, \quad -\Delta_{^2\mathrm{nD}} + m_e \leqslant E_\nu, \tag{16b}$$

$$^2n + \bar{e} \leftrightarrow \mathrm{D} + \bar{\nu}_e, \quad \Delta_{^2\mathrm{nD}} + m_e \leqslant E_\nu, \tag{16c}$$

$$^2n + \bar{e} + \nu_e \leftrightarrow \mathrm{D}, \quad 0 \leqslant E_\nu \leqslant -\Delta_{^2\mathrm{nD}} - m_e, \tag{16d}$$

where we have denoted by $\Delta_{^2\mathrm{nD}}$ the dineutron-deuteron mass difference i.e $\Delta_{^2\mathrm{nD}} = \Delta_{\mathrm{np}} + B_\mathrm{D} - B_{^2\mathrm{n}} = 3.52\ \mathrm{MeV} - B_{^2\mathrm{n}}$. We do not consider those cases where the final states are free nucleons. From the limits on the neutrino energy, E_ν, we see that, at most, only three of these reactions can be operant at any given value of $B_{^2\mathrm{n}}$. For $B_{^2\mathrm{n}} \geqslant 3.01$ MeV the dineutron is stable and for $B_{^2\mathrm{n}} \geqslant 4.03$ MeV the deuteron is unstable.

For these rates we use expressions similar to the neutron-proton interconversion rates but with different Q values and a matrix element that takes into account the presence of two neutrons. We also use a pure Gamow-Teller decay between the 0^+ ground state of the dineutron and the 1^+ ground state of the deuteron or vice versa. While there remains some uncertainty in the rates it has a much smaller impact on final abundance yields as compared with the uncertainties in the strong interaction rates discussed above.

There is an interesting quirk that appears when $\Delta_{^2\mathrm{nD}} < m_e$, which is that an atom of deuterium can capture an electron to form a dineutron. Although interesting this process has not been included in our calculations because the amount of atomic deuterium is negligible at the temperatures relevant to BBN.

$n(n,\gamma)^2n$ and $^2n(p,\gamma)T$

Though $n(n,\gamma)^2n$ looks similar to deuteron formation via $n(p,\gamma)\mathrm{D}$ this reaction is suppressed because there is no charge. Despite this smallness, it is the only exothermic reaction capable of producing dineutrons when $B_{^2\mathrm{n}}$ is small. Following Rupak [63], the lowest order contribution to this cross section should be something like $(N^T\sigma_2 \otimes \tau_2\tau_j N)^\dagger (N^T\sigma_2 \otimes \tau_2\tau_j(\tilde{D}_k + \vec{D}_k)N)E_k$ and $(N^T\sigma_2 \otimes \tau_2\tau_j N)^\dagger (N^T\sigma_2\sigma_i \otimes \tau_2\tau_j(\tilde{D}_k - \vec{D}_k)N)B_l\epsilon^{ikl}$. From examining the $n(p,\gamma)\mathrm{D}$ operators in the cross section from Rupak we estimated that this lowest order contribution is $\mathrm{N^4LO}$. We therefore make an order of magnitude estimate for the dineutron cross section by starting with the $n(p,\gamma)\mathrm{D}$ (which has a leading order contribution) and suppressing it by the appropriate factor. Although there is considerable error, just as with the two $^3\mathrm{He} + {}^2n$ reactions, the effects of the dineutron will only become apparent when $B_{^2\mathrm{n}}$ approaches B_D by which time this reaction will be of little importance.

The $^2n(p,\gamma)\mathrm{T}$ reaction has been included as a failsafe mechanism to remove dineutrons since it is exothermic for all $B_{^2\mathrm{n}}$. It is not expected to be an important reaction unless we strongly deviate from the nucleon flow in standard BBN because the similar, standard BBN reaction $\mathrm{D}(n,\gamma)\mathrm{T}$ is also unimportant. We have also estimated its cross section from the $n(p,\gamma)\mathrm{D}$ reaction in [63] after modifying the phase space and spin multiplicity factors using the expressions discussed above.

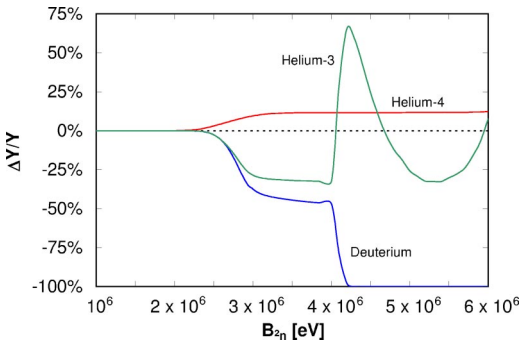

FIG. 2. The fractional change in the primordial deuterium, helium-3 and helium-4 abundances as a function of the dineutron binding energy.

IV. THE EFFECTS OF A BOUND DINEUTRON UPON BBN

The chief manner in which the dineutron affects BBN is via the Q values for the reactions and, from the values quoted earlier, we can identify four regions of $B_{^2\mathrm{n}}$ up to the 6 MeV limit we considered. They are:

$$B_{^2\mathrm{n}} \leqslant B_\mathrm{D},$$
$$B_\mathrm{D} \leqslant B_{^2\mathrm{n}} \leqslant 3.0\ \mathrm{MeV},$$
$$3.0\ \mathrm{MeV} \leqslant B_{^2\mathrm{n}} \leqslant 4.0\ \mathrm{MeV},$$

and

$$4.0\ \mathrm{MeV} \leqslant B_{^2\mathrm{n}}.$$

In Fig. 2 we plot the fractional change in the primordial abundance relative to standard BBN at $\eta = 6.14 \times 10^{-10}$ and the four regions we have identified are clearly visible. Up to B_D there is no discernable change with $B_{^2\mathrm{n}}$, over the interval $B_\mathrm{D} \leqslant B_{^2\mathrm{n}} \leqslant 3.0$ MeV the deuterium and helium-3 abundances drop and the helium-4 abundance rises but after 3.0 MeV the helium-3 and helium-4 abundances plateau and the evolution of Y_D changes noticeably. At 4.0 MeV new behavior emerges: the deuterium abundance drops precipitously while at the same $B_{^2\mathrm{n}}$ there is a large enhancement in helium-3. Most interestingly helium-4 appears to be unaffected by whatever mechanism is producing the wild swings in the other two nuclei.

In what follows we shall explain why and how the dineutron influences BBN in each region.

A. $B_{^2\mathrm{n}} \leqslant B_\mathrm{D}$

For $B_{^2\mathrm{n}} \ll B_\mathrm{D}$ the dineutron lifetime is of order 1 s so while the decay would appear to be a significant drain on the dineutron abundance any loss is easily, and rapidly, replaced from the pool of free neutrons and, consequently, the dineutron abundance during the second stage of BBN follows its NSE value:

$$Y_{^2\mathrm{n}} = \frac{1}{3}\frac{Y_\mathrm{n} Y_\mathrm{D}}{Y_\mathrm{p}} \exp\left(\frac{B_{^2\mathrm{n}} - B_\mathrm{D}}{T}\right). \tag{17}$$

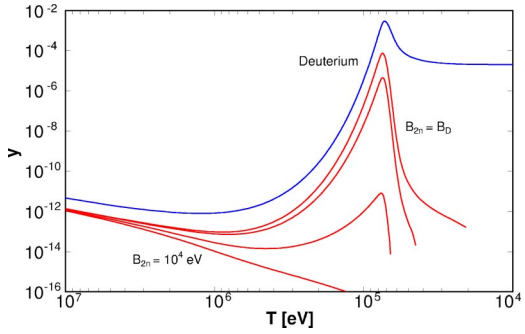

FIG. 3. The evolution of the dineutron abundance as a function of the temperature for $B_{2_n} \in \{10^4 \text{ eV}, 10^6 \text{ eV}, 2\times 10^6 \text{ eV}, B_D\}$ and the deuteron abundance from standard BBN.

Therefore the effect of increasing the dineutron binding energy is the same as one expects from NSE, i.e. the abundance builds up at higher temperature as the binding energy increases. The evolution of the dineutron abundance as a function of the temperature for the four cases $B_{2_n} \in \{10^4 \text{ eV}, 10^6 \text{ eV}, 2\times 10^6 \text{ eV}, B_D\}$ is shown in Fig. 3. In every example in the figure the dineutron abundance is smaller than the deuteron abundance: even when $B_{2_n} = B_D$ the NSE abundance is smaller than Y_D due to both the smaller abundance of free neutrons ($Y_n/Y_p \sim 1/6 - 1/7$) and the spin factor, 1/3, of deuterons, combining for a total of $\sim 1/20$. The figure also makes it quite clear that as B_{2_n} approaches B_D the dineutron starts to possess a considerable abundance at the transition to BBN proper, approximately the location of the deuteron peak. And the figure also shows that the position of the peak dineutron abundance is unaffected by its binding energy and is coincident with the deuteron peak. Whatever the dineutron binding energy in this range BBN proper is still initiated by the deuteron's departure from NSE and the small amount of dineutrons present at that time is rapidly removed. When $B_{2_n} \ll B_D$ their small abundance means that they never form a substantial population which could possibly influence the predictions of BBN but as B_{2_n} approaches B_D their presence at T_{BBN} becomes important.

B. $B_D \leqslant B_{2_n} \leqslant 3.0$ MeV

As shown above, the NSE dineutron abundance at $T \sim 100$ keV when $B_{2_n} = B_D$ is smaller than Y_D by roughly a factor of 1/20 so it is not until the dineutron binding energy has grown to the point where it is capable of reversing the suppression of its NSE abundance by the neutron-to-proton ratio and the spin of the deuteron that its abundance approaches Y_D at $T \sim 100$ keV. Roughly this occurs when

$$\exp\left(\frac{B_{2_n} - B_D}{T}\right) \sim 20, \tag{18}$$

i.e., when $B_{2_n} \sim 2.5$ MeV. The evolution of the dineutron and deuteron abundances during this interval for B_{2_n} is shown in Fig. 4 and confirms that the dineutron abundance surpasses the deuteron abundance at $B_{2_n} \sim 2.5$ MeV. The figure also demonstrates a number of new features: the position of the dineutron peak abundance now moves to higher temperatures

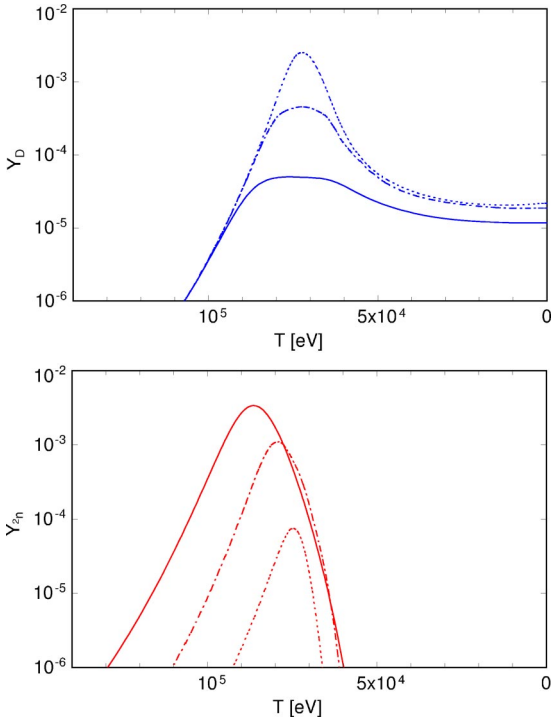

FIG. 4. The evolution of the deuterium (top panel) and dineutron (bottom panel) abundances as a function of the temperature for $B_{2_n} \in \{B_D$ (dotted line), 2.6 MeV (dot-dashed line), 3 MeV (solid line)$\}$.

as B_{2_n} increases, the peak deuterium abundance drops and the temperature at which it departs NSE also shifts to higher temperatures. These effects ripple through to the triton and helion as shown in Fig. 5. As B_{2_n} increases tritium and helium-3 depart NSE at lower temperatures: the change is not dramatic, by $B_{2_n} = 3$ MeV the two $A = 3$ nuclei depart at $T \sim 170$ keV rather than at around 200 keV in standard BBN but the sensitivity of the NSE abundance to the temperature means that the abundance of helium-3 and tritium after this point is roughly 2–3 orders of magnitude larger. The figure also shows that the movement of the tritium peak parallels that for dineutrons by shifting to higher temperatures as B_{2_n} increases.

The movements in the abundances of the intermediary nuclei are all attributable to changes in the flow of the nuclei through the reaction network. For $B_{2_n} \geqslant B_D$, the reaction $\mathrm{D}(n,p)^2 n$ is now exothermic and a detailed examination of the nuclear flow at $B_{2_n} = 2.6$ MeV confirms this to be the source of dineutrons. The flow also indicates the dineutrons are then chiefly converted to tritons via the reaction $^2 n(\mathrm{D},n)\mathrm{T}$. Both reactions lead to a disruption of the usual mechanisms that lead to BBN proper. In standard BBN the transition to BBN proper was due to the removal of deuterons via the two D+D processes but now, because beyond $B_{2_n} \sim 2.5$ MeV the NSE abundance of dineutrons is *larger* than that of deuterons and because free neutrons are so plentiful during the second stage of BBN, the departure occurs earlier. Remarkably both $\mathrm{D}(\mathrm{D},n)^3\mathrm{He}$ and $\mathrm{D}(\mathrm{D},p)\mathrm{T}$ are now of little consequence. The shift in the deuteron's NSE departure temperature is not large, Fig. 4 demonstrates this, but, as

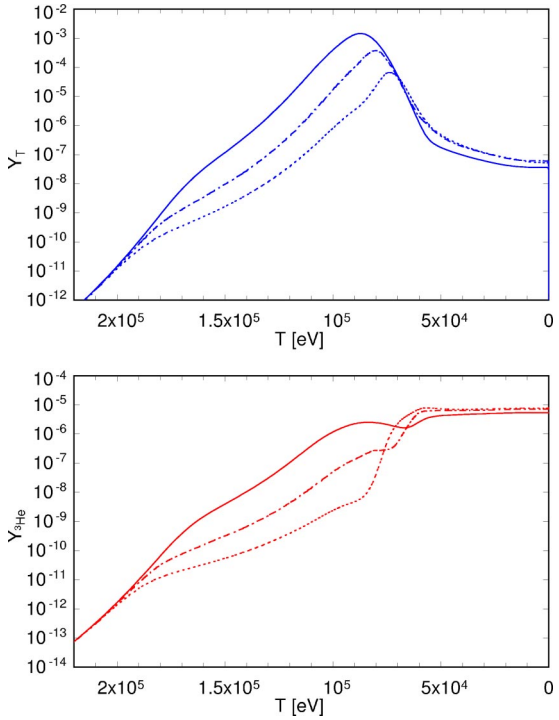

FIG. 5. The evolution of the tritium (top panel) and helium-3 (bottom panel) abundances as a function of the temperature for $B_{2_n} \in \{B_D$ (dotted line), 2.6 MeV (dot-dashed line), 3 MeV (solid line)$\}$.

with T and ^{3}He, the deuteron's NSE abundance is very sensitive to the temperature. The ^2n(D,n)T reaction can also provide sufficient tritium to keep its abundance in equilibrium until a slightly lower temperature. The switch in the mechanism that initiates BBN proper explains many of the features seen in Figs. 4 and 5.

From the nuclear flow we also find that helium-3 no longer plays an important role in the formation of helium-4. Some helium-3 is still formed, via D(D,n)^{3}He, but this source is suppressed due to the lack of deuterons; what little helium-3 is created is processed to tritium by the usual ^{3}He(n,p)T though ^{3}He(^2n,n)^{4}He does play a role. The reduced significance of helium-3 is not reflected in Fig. 5: one must remember that the net rate of formation for the intermediary D, T and ^{3}He is the small difference between production and destruction and does not necessarily indicate the true amount of nucleons flowing through them. Even in standard BBN the evolution of helium-3 does not resemble that of tritium because ^{3}He(n,p)T is so rapid and one can only see the significance of the helium-3 nucleus by examining the individual reaction rates [54].

Finally, the formation of helium-4 still occurs via T(D,n)^{4}He and, due to the earlier initiation of BBN proper, its final (primordial) abundance is enhanced. The reaction network is modified and the bulk of the nucleons now flow through a network resembling that shown in Fig. 6.

By $B_{2_n}=3$ MeV Fig. 4 shows that the peak abundance of deuterons has dropped by two orders of magnitude from that in standard BBN and BBN proper begins at an even higher temperature. The nuclear flow now indicates that tritium formation is increasingly dominated by ^2n(p,γ)T rather than ^2n(D,n)T and, interestingly, the dominant source of helium-3 is the mildly endothermic T(p,n)^{3}He at higher temperatures with a changeover to T(D,^2n)^{3}He as the Universe cools. This flow, T(p,n)^{3}He, is opposite to that in standard BBN, ^{3}He(n,p)T.

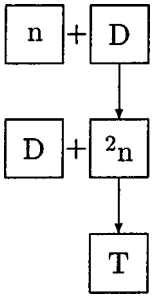

FIG. 6. The schematic flow of nuclei through the reaction network from deuterium to tritium at $B_{2_n}=2.6$ MeV. The flow does not include helium-3. A little of this nucleus is still produced via D(D,n)^{3}He but the suppressed deuteron abundance means that the amount is substantially reduced compared to standard BBN.

This second region of B_{2_n} is where the presence of dineutrons really becomes manifest. At $B_{2_n}=B_D$ the dineutron is just starting to influence BBN, by $B_{2_n}=3$ MeV it has considerably altered the reaction network that take the free neutrons to helium-4 and led to a significant change in the mechanism that leads to BBN proper.

C. 3.0 MeV$\leqslant B_{2_n} \leqslant$4.0 MeV

The excitement seen when $B_D \leqslant B_{2_n} \leqslant 3$ MeV has largely played out as we enter the third domain of 3 MeV$\leqslant B_{2_n} \leqslant$4.0 MeV and the shifts in the evolution of the abundances slows. In this range, between 3 and 4 MeV, there are no new, major changes in the nuclear flow because the Q values of the most important reactions are now all $\sim$MeV. Nevertheless, a detailed study of the reaction network does show small differences and we discuss those here.

Although further increases in the dineutron binding energy are not reflected in the position and amplitude of the peak dineutron abundance, the temperature at which the dineutron departs NSE shifts to higher values with B_{2_n}. In contrast, the reduction in the amplitude of the peak deuteron abundance seen in Fig. 4 becomes less dramatic and its NSE departure temperature has all but ceased to move as B_{2_n} increases.

The behavior of the evolution of these two $A=2$ nuclei reflect the fact that dineutrons are primarily created from deuterons and that the dominant dineutron destruction mechanism has switched from ^2n(D,n)T to ^2n(p,γ)T. Dineutron NSE departure occurs because of insufficient production from the small D abundance. The ^2n abundance at lower temperatures is thus controlled by the deuteron. The reaction ^2n(p,γ)T is affected by B_{2_n} only through the exit channel phase space which varies as $\sqrt{B_T - B_{2_n}}$. With an abundance controlled by D and a destruction mechanism that varies only weakly with B_{2_n} the height and temperature of the peak dineutron abundance is, essentially, static. Deute-

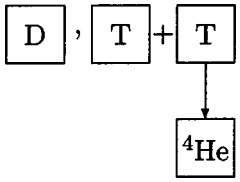

FIG. 7. The diagrammatic flow of nuclei through the reaction network from tritium onwards at $B_{2_n}=3.5$ MeV.

rium departure from NSE occurs when its abundance opens the $D(n,p)^2n$ drain and, again, B_{2_n} only enters weakly through the exit channel phase space.

A new feature emerges in this third region of B_{2_n}. At $B_{2_n}\geqslant 3.0$ MeV, the Q value for the reaction $^3He(^2n,D)T$ is now negative and the importance of the helion as an intermediary in the formation of helium-4 rebounds, though not to the level in standard BBN. The source of helions is principally the mildly endothermic $T(p,n)^3He$ but switches to $T(D,\ ^2n)^3He$ as the Universe cools.

Finally, helium-4 is now chiefly formed by both $T(D,n)^4He$ and $T(T,2n)^4He$ in almost equal proportions with minor contributions from $T(p,\gamma)^4He$ and $^3He(^2n,n)^4He$. The network has changed slightly and the new flow at $B_{2_n}=3.5$ MeV is illustrated in Fig. 7.

D. 4.0 MeV$\leqslant B_{2_n}$

As B_{2_n} enters this last region we identified from Fig. 2 there is a dramatic drop in the final deuterium abundance, a large spike in the helium-3, and no change in the helium-4 until B_{2_n} approaches 6 MeV. The explanation for this behavior lies in the instability of the deuteron when $B_{2_n}\geqslant 4$ MeV and the lack of Coulomb barriers in dineutron reactions. Deuteron decay to dineutrons removes the possibility of a relic D abundance while, as we explained earlier, reactions without Coulomb barriers [$^2n(p,\gamma)T$ and $^3He(^2n,n)^4He$ for example] can continue indefinitely. For $B_{2_n}\geqslant 4$ MeV the primordial $A=2$ abundance is negligible.

When B_{2_n} is only slightly larger than 4 MeV deuteron decay occurs long after the Coulomb barriers have become effective so that only $^2n(p,\gamma)T$ and $^3He(^2n,n)^4He$, together with deuteron and triton, decay operate. The evolution of the nuclei during this ''post-BBN'' period is by no means clear-cut. From studying the nuclear flow we find that only a few dineutrons are lost via $^3He(^2n,n)^4He$, the majority is destroyed by $^2n(p,\gamma)T$. The extra tritons more than compensate for the loss of helium-3 and so the $A=3$ isobar receives a large boost. But as B_{2_n} increases the deuterons decay earlier permitting the $T(D,n)^4He, T(T,2n)^4He, T(p,\gamma)^4He$ reactions to remove the tritium and so there is a small enhancement in helium-4.

As the ^2n binding energy is pushed towards 6 MeV the Q value in the reaction (5) approaches the temperatures during BBN and we should expect new modifications to the nucleon flow diagrams but, with no possibility of a $A=2$ primordial abundance, we shall not pursue this further.

V. ARE THESE PREDICTIONS ROBUST?

While we have strived to estimate the various dineutron cross sections by basing them upon simple physical assumptions, it is a worthwhile task to see how robust the effects we have described are. If we know (or assume) the distribution for the error, either in the cross section or the thermally averaged rate, then one can compute the error matrix as in Fiorentini *et al.* [65] and Cuoco *et al.* [64], though this approach cannot recover higher moments of the abundance distribution. An alternative is to construct the distribution of the abundances by sampling the distribution of the errors in a Monte Carlo analysis. This technique was used by Krauss and Romanelli [66], Smith, Kawano and Malaney [54], Krauss and Kernan [67] and, more recently, Nollett and Burles [68] and is the technique we shall use. To this end we introduced random multiplicative factors for all our dineutron reaction cross sections with the exception of $^2n\leftrightarrow D$, the most reliably estimated. These factors were chosen from a probability distribution limited to the range between 1/5 and 5 and weighted such that there was equal probability either side of 1. The baryon-to-photon ratio was fixed at $\eta=6.14\times10^{-10}$. In Fig. 8 we plot the root mean square deviations for deuterium and helium-4 and the three regimes for the dineutron binding energy (up to the 4 MeV limit plotted) are clearly visible in both curves. The increasing spread for both reflects the increasing dominance of dineutron reactions in the formation of helium-4. The figure shows that up to $B_{2_n}\sim 2$ MeV the errors in the reactions involving dineutrons do not introduce any error into the predicted abundances, illustrating again the insignificance of dineutrons in BBN when their binding energy is smaller than this value. Above $B_{2_n}\sim 2$ MeV the curves begin to deviate from zero but note two important features: first, the spread in helium-4 is small for all values of B_{2_n}, and second, the spread in the predicted abundance of deuterium does not exceed $\pm 100\%$. The small spread in the helium-4 curves indicate that we can reliably predict the abundance of helium-4 even if dineutrons have significantly impacted BBN, while the fact that the deuterium curves do not exceed 100% shows that at least the *direction* of the change is known even if the exact abundance is not. We have not shown the rms spread for helium-3 because it exceeded $\pm 100\%$.

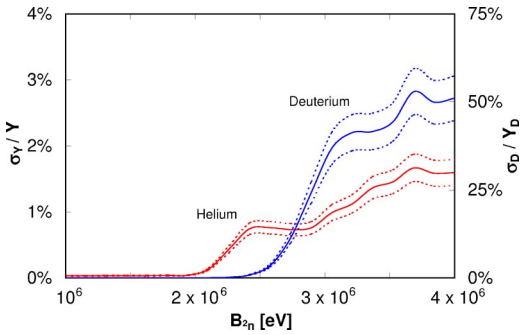

FIG. 8. The root mean square deviation divided by the mean plus the $\pm 3\sigma$ error for deuterium and helium-4 as a function of the dineutron binding energy. Below $B_{2_n}\sim 2$ MeV neither nucleus exhibits any spread due to the uncertainty in the dineutron reaction rates. Above this value the spread in the deuterium results becomes large while the results for helium remain smaller than $\sim 2\%$ for all value of B_{2_n}.

Note also that the range in the abundances is significantly

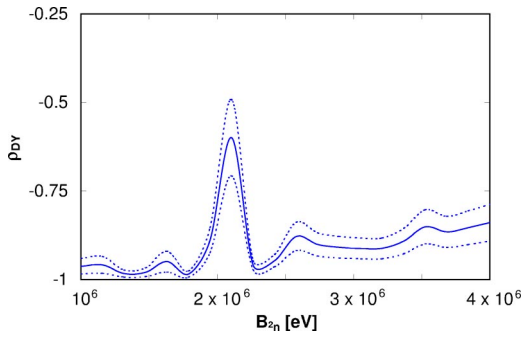

FIG. 9. The correlation between the deuterium abundance and helium-4 mass fraction, ρ_{DY}, and its $\pm 3\sigma$ error, as a function of the dineutron binding energy. Below $B_{2\mathrm{n}} \sim 2$ MeV the correlation is close to -100% while after $B_{2\mathrm{n}} \sim 3$ MeV the correlation has softened to $\sim -80\%$. The large peak at $B_{2\mathrm{n}} \sim 2$ MeV corresponds to the point where the change in the flow of nuclei through the reaction network occurs.

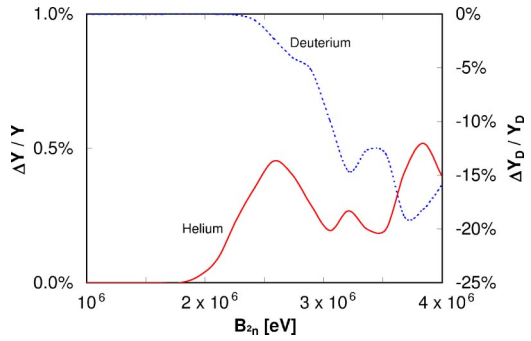

FIG. 10. The fractional difference between the mean from the Monte Carlo simulation and the result with no random factors. The solid line is for helium-4, the dotted is for deuterium.

smaller than the range we permitted for the random factors. This may seem remarkable since the primordial abundance of an intermediary nuclei, such as deuterium, involves a fierce competition between its production and destruction and hence the adopted cross sections. While dineutrons may have led to significant departures in the flow of nuclei compared to standard BBN, large variations in the dineutron reaction rates do not translate into equally large spreads in the abundances of the intermediaries.

We also found that there was a significant anticorrelations in the results as shown in Fig. 9. For $B_{2\mathrm{n}} \lesssim 2$ MeV the correlation coefficient was almost exactly -1 while over the interval $2.5\ \mathrm{MeV} \lesssim B_{2\mathrm{n}} \lesssim 3\ \mathrm{MeV}$ the anticorrelation softened slightly to ~ -0.8. As a consequence of this correlation the covariance matrix, V_R, describing the error in the predictions arising from the uncertainties in the dineutron's reaction rates, contains off-diagonal pieces.

We have delayed until last the difference we find in the mean from the sample and the primordial abundances we derive with no random factors as shown in Fig. 2. The fact that a discrepancy arises is not surprising given the nonlinearity of BBN. The errors (which are functions of $B_{2\mathrm{n}}$) for helium-4 is $\lesssim 0.5\%$ but for deuterium it reaches $\lesssim 20\%$ and helium-3 fared even worse with a discrepancy between the mean and no random factors approaching 30%. The fractional difference between the mean and the result with no random factors are shown in Fig. 10 for deuterium and helium-4. Although seemingly large, this error is smaller than the statistical fluctuations for all three nuclei (seen in Fig. 8 for deuterium and helium-4) but not significantly so and we must include it in the total error for the predictions as a systematic. The covariance matrix for the systematic error is denoted by V_S.

With means, $\overline{\mathbf{Y}}$, and variance, $V_T = V_R + V_S$, that are functions of $B_{2\mathrm{n}}$ we approximate the distributions in the predictions as Gaussians

$$P(\mathbf{Y}|B_{2\mathrm{n}}) = \frac{1}{\sqrt{2\pi|V_T|}} \exp\left[-\frac{1}{2} (\mathbf{Y} - \overline{\mathbf{Y}})^T V_T^{-1} (\mathbf{Y} - \overline{\mathbf{Y}}) \right]. \tag{19}$$

We have checked the validity of this approximation to the spread in the results by performing a Kolmogorov test at each value of $B_{2\mathrm{n}}$ we set. The spread in the predictions for helium-3, which we have not shown, did not pass this due to a significant kurtosis.

VI. A DEGENERACY WITH η?

So far we have restricted our discussions to a fixed value of the baryon-to-photon ratio, η, but if we allow this parameter to also vary we may well end up with a degeneracy that makes it difficult to establish the presence of a bound dineutron. To determine if this occurs, we show in Fig. 11 iso-abundance and iso-mass fraction contours for deuterium and helium respectively as a function of $B_{2\mathrm{n}}$ and η. If we examine the most robust prediction of our modified BBN, the increase in Y, then we can quite easily mask this effect by *lowering* η as shown in the figure. The decrease in η required to offset the increase in the primordial mass fraction as $B_{2\mathrm{n}}$ increases is considerable so that above $B_{2\mathrm{n}} \sim 2.5$ MeV all values of η in the 3×10^{-10} to 8×10^{-10} range plotted yield a helium-4 mass fraction above 0.248. For deuterium, lower values of η lead to increases in the final abundance so that they too can mitigate the decrease in Y_{D} as $B_{2\mathrm{n}}$ increases. But the figure shows that the decrease in η required for deuterium is nowhere near as large as that

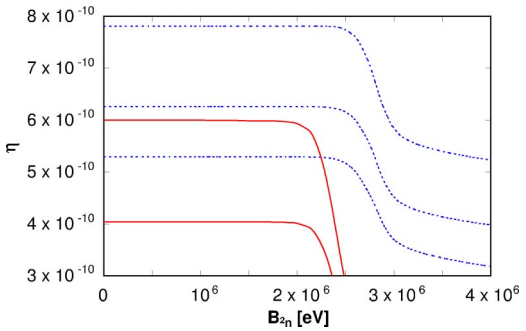

FIG. 11. Helium-4 iso-mass fraction (solid) and Deuterium iso-abundance (dashed) contours in the $B_{2\mathrm{n}} - \eta$ plane. From top to bottom, the helium-4 contours are $Y = 0.248$ and $Y = 0.244$ and the deuterium abundances are $\mathrm{D/H} = 1.8 \times 10^{-5}$, $\mathrm{D/H} = 2.6 \times 10^{-5}$ and $\mathrm{D/H} = 3.4 \times 10^{-5}$.

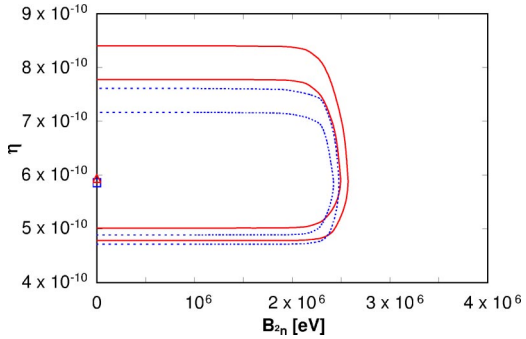

FIG. 12. The 95% and 99% confidence contours using the Olive, Steigman and Walker (solid curves) and Izotov and Thuan (dashed curves) helium-4 mass fractions observations and the Barger *et al.* [14] primordial deuterium abundance. The best fit points, both at $B_{2_n}=0$, are denoted by the triangle for OSW, the square for IT.

required for helium-4, so, while there is an anticorrelation of B_{2_n} and η for both helium-4 and deuterium, there is no degeneracy for both simultaneously. If we considered each species separately then the degeneracy could, instead, be broken by using the CMB since lowering η_{BBN} will lead to a discrepancy with η_{CMB}.

VII. AN UPPER LIMIT FOR B_{2_n}

It is finally time to derive an upper limit to B_{2_n} based on the compatibility with observations. The primordial abundance, D/H, of deuterium is taken to be $\mathrm{D/H}=(2.6\pm0.4)\times10^{-5}$ [14] while we will consider both the Olive, Steigman and Walker [71] value of $Y_{OSW}=0.238\pm0.005$ and the Izotov and Thuan value of $Y_{IT}=0.244\pm0.002$ [72,73] for the helium-4 mass fraction Y. The exact primordial abundances remain a topic of debate with two, largely incompatible, determinations for the helium mass fraction [72–76] and excessive scatter in the measurements of deuterium [14,77] but these two nuclei still represent the best probes of BBN.

The error in the observed helium-4 mass fractions are 2% for Y_{OSW}, 1% for Y_{IT} which compares well with the spread in the predicted mass fraction plotted in Fig. 8. We can integrate over the possible values for the prediction, at a fixed η and B_{2_n}, using the distributions found earlier, and find

$$\mathcal{L}(\eta,B_{2_n}|\hat{\mathbf{Y}})=\frac{1}{\sqrt{2\pi|V|}}\exp\left[-\frac{1}{2}(\hat{\mathbf{Y}}-\mathbf{Y})^T V^{-1}(\hat{\mathbf{Y}}-\mathbf{Y})\right], \tag{20}$$

where $\hat{\mathbf{Y}}$ denotes the vector whose elements are the observations and $\mathbf{Y}$ the vector whose elements are the predictions and V is the covariance matrix—the sum of the (diagonal) covariance matrix for the observations, V_O, and the two covariance matrices V_R and V_S. Contours of the likelihood are shown in Fig. 12 which shows that the use of deuterium and helium-4 breaks the degeneracy seen in each separately, and, indeed, the limits to the dineutron binding energy are independent of the baryon-to-photon ratio.

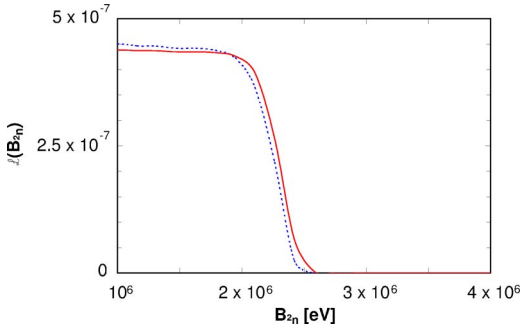

FIG. 13. The marginalized likelihood function for B_{2_n} using the Olive, Steigman and Walker (solid curve) and Izotov and Thuan (dashed curve) helium-4 mass fractions observations and the Barger *et al.* [14] primordial deuterium abundance.

Marginalizing over the baryon-to-photon ratio, η, we obtain the results shown in Fig. 13. The two upper limits for B_{2_n} are not greatly influenced by the different primordial helium-4 mass fractions found in the literature.

VIII. SIMULTANEOUS VARIATIONS IN B_D

Throughout our calculation so far we have only permitted the variation of the dineutron binding energy. In reality, whatever the source of the stability of the dineutron, naively the binding energies of the other nuclei should also change. The range in B_{2_n} we investigated is much larger than the range in B_D that Kneller and McLaughlin permitted but we notice that the increase in Y and decrease in D/H seen there when B_D increased is also mimicked by an increase in the dineutron binding energy when $B_{2_n}\gtrsim B_D$.

To investigate the effects when both B_D and B_{2_n} are varied we reproduced the Kneller and McLaughlin calculation but now with dineutrons inserted. Tritons and helions act as the neutron sinks in this simplified BBN so reactions (6a) and (6b) have to be removed from the network. The results are shown in Fig. 14. The primordial helium-4 mass fraction

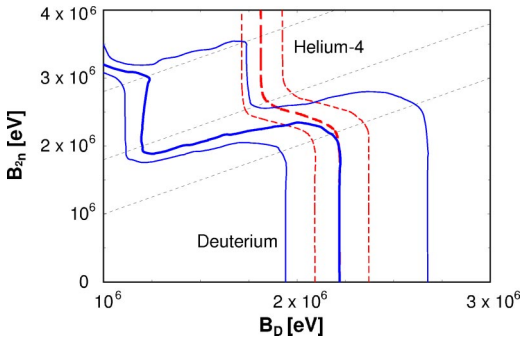

FIG. 14. Contours of deuterium iso-abundance (solid) and helium-4 iso-mass fraction (dashed) as a function the deuteron binding energy, B_D, and dineutron binding energy, B_{2_n}. The abundances are scaled relative to their values at $B_D=2.22$ MeV and $B_{2_n}=0$ to remove the systematic errors coming from the reaction network simplification. From left to right the deuterium contours are +30%, 0% and −30% while the helium-4 contours are −4.2%, 0% and +4.2%. The three diagonal lines are the linear equations $B_{2_n}=B_D$, $B_{2_n}=B_D+0.8$ MeV and $B_{2_n}=B_D+1.8$ MeV.

from the Kneller and McLaughlin approximations is known to be systematically low by ~1% when compared to standard BBN calculations but this is within the observational errors on Y. The deuteron abundance is systematically large by ~50% which is significantly larger than the observational error of 15%. For this reason we have scaled both the helium-4 and deuteron abundances to the values at $B_D = 2.22$ MeV and $B_{2n} = 0$. The contours in the figure represent relative differences of ±30% for deuterium and ±4.2% for helium-4 indicating the degree to which the errors in the observations can constrain simultaneous variations. The diagonal lines through the figure are the linear relations $B_{2n} = B_D$, $B_{2n} = B_D + 0.8$ MeV and $B_{2n} = B_D + 1.8$ MeV and generalize the four domains of B_{2n} when $B_D = 2.22$ MeV seen in Fig. 2 into the $B_{2n} - B_D$ plane.

Features discussed in earlier sections of this paper generalize to simultaneous variations of B_D and B_{2n}. At any fixed B_D there are four ranges for B_{2n} and for two of these, $B_{2n} \leqslant B_D$ and $B_D + 0.8\ \text{MeV} \leqslant B_{2n} \leqslant B_D + 1.8$ MeV, the predictions for helium-4 and deuterium are independent of B_{2n} even though the flow of nuclei in each is different. For $B_{2n} \leqslant B_D$ BBN is initiated by the D+D drain upon the deuteron abundance while for dineutron binding energies between $B_D + 0.8$ MeV and $B_D + 1.8$ MeV this has switched to D $+ {}^2n$. In the range $B_D \leqslant B_{2n} \leqslant B_D + 0.8$ MeV the reaction network is transiting between these two patterns. Lastly, for $B_D + 1.8\ \text{MeV} \leqslant B_{2n}$ we have the domain in which the deuteron is unstable.

The figure shows that if B_D and B_{2n} increase in tandem then the stability of the dineutron cannot reverse the increase in Y whatever the relative magnitudes of the two binding energies and even though dineutrons may alter the nucleon flow. If these two binding energies change in opposite senses then the situation is more interesting: the effect of a decrease in B_D is the immediate decrease in the helium-4 mass fraction so that for $B_{2n} \leqslant B_D$ the deuteron binding energy cannot vary by more than 6% from its present value. The presence of the dineutron can reverse the decrease in Y only when $B_{2n} \geqslant B_D$. Even then B_D is well constrained and deuteron binding energies smaller than 1.7 MeV are incompatible with the helium-4 mass fraction observations whatever the value of B_{2n}. The deuterium contours tell a similar story but the effects of a stable dineutron are more pronounced and the decrease in B_D is much larger. Taken together the observations of the primordial helium-4 mass fraction and deuteron abundance are only compatible with the BBN predictions with dineutron binding energies above ~2.5 MeV when the deuteron binding energy is close to $B_D \sim 1.7$ MeV. In these circumstance the upper limit moves to 3.5 MeV and is set by the decay of the deuteron.

IX. SUMMARY AND CONCLUSIONS

We have examined the role that a stable dineutron may play in BBN as a function of its binding energy, B_{2n}, up to 6 MeV. We have estimated the important new reactions that enter into the BBN reaction network and examined, in detail, the change in the nucleon flow. We find that the range $0 \leqslant B_{2n} \leqslant 6$ MeV can be subdivided into four regions: $B_{2n} \leqslant B_D$, $B_D \leqslant B_{2n} \leqslant 3$ MeV, 3 MeV $\leqslant B_{2n} \leqslant 4$ MeV and 4 MeV $\leqslant B_{2n}$. The boundaries are due to the sign inversion of the ${}^2n(p,n)\text{D}$ and ${}^3\text{He}({}^2n,\text{D})\text{T}$ Q values and the spontaneous decay of the deuteron. Below B_D the dineutron has little effect upon BBN but as we increased B_{2n} beyond this value nucleons began to flow through the new reaction pathways the dineutron presents. The helium-4 mass fraction increased by ~10% and the deuterium abundance dropped by ~40%. Between 3 and 4 MeV the nucleon flow settled into a new pattern, the helium-4 mass fraction plateaued to new level and the rate at which the deuterium abundance decreases with B_{2n} slowed. A small change to the nucleon flow from tritium to helium-4 was seen.

Above 4 MeV the deuteron is now unstable and a significant primordial $A = 2$ abundance cannot be produced. If deuterons decay long after Coulomb barriers have essentially terminated charged particle reactions this can lead to a large boost in the $A = 3$ abundance but as the interval shortens this enhancement is removed and the nucleons continue on to helium-4.

We estimated the error in the predictions by sampling the distribution of abundances when the dineutron reactions were multiplied by random factors and found that the predictions of an increase in the helium-4 mass fraction and decrease in deuteron abundance were reliable. The degeneracy between B_{2n} and the baryon-to-photon ratio, η, that occurs for Y and D/H separately was broken when both were considered simultaneously. We then constructed the 2-D likelihood function $\mathcal{L}(\eta, B_{2n} | Y, D/H)$ by using both the OSW [71] and IT [72,73] helium-4 mass fractions and the Barger *et al.* [14] deuterium abundance before marginalizing over η to derive the likelihood distribution for B_{2n}. We found that dineutron binding energies above ~2.5 MeV could not be accommodated by BBN within both allowed ranges of Y.

Simultaneous variations in both the dineutron and deuteron binding energies were calculated using the simplified BBN approximation used in Kneller and McLaughlin [38]. The helium-4 observations are only compatible within a narrow range of B_D whatever the value of B_{2n} and that there is little overlap with the range compatible with the deuterium abundance when $B_{2n} \gtrsim 2.5$ MeV.

In this paper we have shown that the dineutron can become bound at a level up to that of the deuteron without disrupting the standard nuclear flow in BBN or significantly altering predicting BBN abundance yields. Beyond that, changes to the nuclear flow and to predicted abundance yields appear. Although we have not included any dineutron reaction involving nuclei with mass above $A = 4$, one can speculate that the omitted reaction ${}^7\text{Be}({}^2n, n\alpha){}^4\text{He}$ could play a significant role since beryllium-7 (before it decays to ${}^7\text{Li}$) is the chief component of the primordial $A = 7$ isobar yield at $\eta \sim 6 \times 10^{-10}$. Further work on the interdependence of cross sections and binding energies in nuclear theory would be required to reduce the errors presented here and to make a more concrete connection with the underlying fundamental constants.

ACKNOWLEDGMENTS

The authors would like to thank Eric Braaten for useful discussions. This work was supported by the U.S. Department of Energy under grant DE-FG02-02ER41216.

[1] D. N. Schramm, Space Sci. Rev. **84**, 3 (1998).
[2] E. Vangioni-Flam, A. Coc, and M. Cassé, Nucl. Phys. **A718**, 389 (2003).
[3] G. Steigman, D. N. Schramm, and J. R. Gunn, Phys. Lett. **66B**, 202 (1997).
[4] J. Yang, D. N. Schramm, G. Steigman, and R. T. Rood, Astrophys. J. **227**, 697 (1979).
[5] E. Lisi, S. Sarkar, and F. L. Villante, Phys. Rev. D **59**, 123520 (1999).
[6] J. P. Kneller *et al.*, Phys. Rev. D **64**, 123506 (2001).
[7] G. Beaudet and A. Yahil, Astrophys. J. **218**, 253 (1977).
[8] R. V. Wagoner, W. A. Fowler, and F. Hoyle, Astrophys. J. **148**, 3 (1967).
[9] H.-S. Kang and G. Steigman, Nucl. Phys. **B372**, 494 (1992).
[10] K. Kohri, M. Kawasaki, and K. Sato, Astrophys. J. **490**, 72 (1997).
[11] K. A. Olive *et al.*, Phys. Lett. B **265**, 239 (1991).
[12] R. J. Scherrer, Mon. Not. R. Astron. Soc. **205**, 683 (1983).
[13] A. Yahil and G. Beaudet, Astron. Astrophys. **206**, 415 (1976).
[14] V. Barger *et al.*, Phys. Lett. B **566**, 8 (2003).
[15] V. Barger *et al.*, Phys. Lett. B **569**, 123 (2003).
[16] A. Serna and R. Dominguez-Tenreiro, Phys. Rev. D **48**, 1591 (1993).
[17] A. Serna, R. Dominguez-Tenreiro, and G. Yepes, Astrophys. J. **391**, 433 (1992).
[18] R. Bean, S. H. Hansen, and A. Melchiorri, Phys. Rev. D **64**, 103508 (2001).
[19] J. P. Kneller and G. Steigman, Phys. Rev. D **67**, 063501 (2003).
[20] X. Chen, R. J. Scherrer, and G. Steigman, Phys. Rev. D **63**, 123504 (2001).
[21] R. Foot, Phys. Rev. D **61**, 023516 (2000).
[22] C. Lunardini and A. Y. Smirnov, Phys. Rev. D **64**, 073006 (2001).
[23] A. D. Dolgov *et al.*, Nucl. Phys. **B632**, 363 (2002).
[24] Y. Y. Wong, Phys. Rev. D **66**, 025015 (2002).
[25] K. N. Abazajian, J. F. Beacom, and N. F. Bell, Phys. Rev. D **66**, 013008 (2002).
[26] M. Kaplinghat, G. Steigman, and T. P. Walker, Phys. Rev. D **61**, 103507 (2000).
[27] E. W. Kolb and R. J. Scherrer, Phys. Rev. D **25**, 1481 (1982).
[28] X. Shi, D. N. Schramm, and B. D. Fields, Phys. Rev. D **48**, 2563 (1993).
[29] X. Shi, G. M. Fuller, and K. Abazajian, Phys. Rev. D **60**, 063002 (1999).
[30] E. W. Kolb, M. J. Perry, and T. P. Walker, Phys. Rev. D **33**, 869 (1986).
[31] J. D. Barrow, Phys. Rev. D **35**, 1805 (1987).
[32] L. Bergstrom, S. Iguri, and H. Rubinstein, Phys. Rev. D **60**, 045005 (1999).
[33] P. P. Avelino *et al.*, Phys. Rev. D **64**, 103505 (2001).
[34] K. M. Nollett and R. E. Lopez, Phys. Rev. D **66**, 063507 (2002).
[35] J. J. Yoo and R. J. Scherrer, Phys. Rev. D **67**, 043517 (2003).
[36] V. V. Flambaum and E. V. Shuryak, Phys. Rev. D **65**, 103503 (2002).
[37] V. V. Flambaum and E. V. Shuryak, Phys. Rev. D **67**, 083507 (2003).
[38] J. P. Kneller and G. C. McLaughlin, Phys. Rev. D **68**, 103508 (2003).
[39] J. K. Webb *et al.*, Phys. Rev. Lett. **82**, 884 (1999).
[40] J. K. Webb *et al.*, Phys. Rev. Lett. **87**, 091301 (2001).
[41] J. N. Bahcall, C. L. Steinhardt, and D. Schlegel, Astrophys. J. **600**, 520 (2004).
[42] T. Ashenfelter, G. J. Mathews, and K. A. Olive, Phys. Rev. Lett. **92**, 041102 (2004).
[43] R. H. Phillips and K. M. Crowe, Phys. Rev. **96**, 484 (1954).
[44] K. Ilakovac *et al.*, Phys. Rev. **124**, 1923 (1961).
[45] W. R. Gibbs, B. F. Gibson, and G. J. Stephenson, Phys. Rev. C **11**, 90 (1975).
[46] O. Schori *et al.*, Phys. Rev. C **35**, 2252 (1987).
[47] B. L. Cohen and T. H. Handley, Phys. Rev. **92**, 101 (1953).
[48] O. V. Bochkarev *et al.*, JETP Lett. **42**, 374 (1985).
[49] O. V. Bochkarev *et al.*, JETP Lett. **42**, 377 (1985).
[50] K. K. Seth and B. Parker, Phys. Rev. Lett. **66**, 2448 (1991).
[51] F. M. Marques *et al.*, Phys. Rev. C **65**, 044006 (2003).
[52] S. R. Beane and M. J. Savage, Nucl. Phys. **A713**, 148 (2003).
[53] S. R. Beane and M. J. Savage, Nucl. Phys. **A717**, 91 (2003).
[54] M. S. Smith, L. H. Kawano, and R. A. Malaney, Astrophys. J., Suppl. Ser. **85**, 219 (1993).
[55] E. Braaten and H. W. Hammer, Phys. Rev. Lett. **91**, 102002 (2003).
[56] W. A. Fowler, G. R. Caughlan, and B. A. Zimmerman, Annu. Rev. Astron. Astrophys. **5**, 525 (1967).
[57] G. Gamow, *Structure of Atomic Nuclei and Nuclear Transformations, second edition of Constitution of Atomic Nuclei and Radioactivity* (Clarendon Press, Oxford, 1937).
[58] H. Bethe, Rev. Mod. Phys. **9**, 69 (1937).
[59] D. D. Clayton, *Principles of Stellar Evolution and Nucleosynthesis* (University of Chicago Press, Chicago, 1983).
[60] G. S. Chulick *et al.*, Nucl. Phys. **A551**, 255 (1993).
[61] http://www.nndc.bnl.gov/nndc/endf/
[62] D. R. Tilley *et al.*, Nucl. Phys. **A708**, 3 (2002), (see also http://www.tunl.duke.edu/nucldata/HTML/HTML_Project.shtml).
[63] G. Rupak, Nucl. Phys. **A678**, 405 (2000).
[64] A. Cuoco *et al.*, astro-ph/0307213.
[65] G. Fiorentini, E. Lisi, S. Sarkar, and F. L. Villante, Phys. Rev. D **58**, 063506 (1998).
[66] L. M. Krauss and P. Romanelli, Astrophys. J. **358**, 47 (1990).
[67] L. M. Krauss and P. Kernan, Phys. Lett. B **347**, 347 (1995).
[68] K. M. Nollett and S. Burles, Phys. Rev. D **61**, 123505 (2000).
[69] J. Bernstein, L. S. Brown, and G. Feinberg, Rev. Mod. Phys. **61**, 25 (1989).
[70] S. Sarkar, Rep. Prog. Phys. **59**, 1493 (1996).
[71] K. A. Olive, G. Steigman, and T. P. Walker, Phys. Rep. **333**, 389 (2000).
[72] Y. I. Izotov, T. X. Thuan, and V. A. Lipovetsky, Astrophys. J., Suppl. Ser. **108**, 1 (1997).
[73] Y. I. Izotov and T. X. Thuan, Astrophys. J. **500**, 188 (1998).
[74] K. A. Olive and G. Steigman, Astrophys. J., Suppl. Ser. **97**, 49 (1995).
[75] K. A. Olive, E. D. Skillman, and G. Steigman, Astrophys. J. **483**, 788 (1997).
[76] B. D. Fields and K. Olive, Astrophys. J. **506**, 177 (1998).
[77] D. Kirkman *et al.*, Astrophys. J., Suppl. Ser. **149**, 1 (2003).